# Coordinating dynamic traffic-power systems under decentralized and centralized decision environments

Hongping Wang, Adam Abdin, Yi-Ping Fang, Jakob Puchinger, Enrico Zio

Computers & Industrial Engineering 196 (2024) 110474

Contents lists available at ScienceDirect

Computers & Industrial Engineering

journal homepage: www.elsevier.com/locate/caie

# Coordinating dynamic traffic-power systems under decentralized and centralized decision environments

Hongping Wang [a,b], Adam Abdin [b], Yi-Ping Fang [b,*], Jakob Puchinger [e,b], Enrico Zio [c,d]

[a] School of Intelligent Engineering and Automation, Beijing University of Posts and Telecommunications, Beijing, China
[b] Université Paris-Saclay, CentraleSupélec, Laboratoire Génie Industriel, 3 rue Joliot-Curie, Gif-sur-Yvette, France
[c] Energy Department, Politecnico di Milano, 20156 Milano, Italy
[d] Mines Paris-PSL, Centre de Recherche sur les Risques et les Crises (CRC), Sophia Antipolis, France
[e] EM Normandie Business School, Métis Lab, 30-32 rue Henri Barbusse, Clichy, 92110, France

ARTICLE INFO

*Keywords:*
Dynamic transportation-power systems
Interactive systems
Electric vehicles
Charging stations
Decision-making environments
Link transmission model

ABSTRACT

This paper proposes a dynamic traffic-electric power network model to investigate the interactions between the power distribution network (PDN) and the electric road network (ERN), whose operations are linked via the local marginal electricity price and the electric vehicles (EVs) charging demand. For the ERN, a novel formulation based on the link transmission model is proposed to: (1) accommodate the critical features of EVs and fast charging stations (FCSs), such as EVs with different driving ranges, initial states of charge of EVs, number of chargers and their charging power in a FCS; (2) explicitly model the charging process of EVs; (3) solve the optimal dynamic traffic assignment problem considering the mix of EVs and gasoline vehicles. For the economic operation of the PDN, an alternating current optimal power flow model is solved to minimize the electricity expenditure. Moreover, we propose mathematical algorithms to describe the interdependent and interactive schemas between the two networks by modeling the decentralized and centralized decision-making environments. The proposed modeling framework is capable of capturing the dynamic interactions that are not possible in classical traffic models. The illustrative traffic-power system shows that decentralized decision-making always results in losses of operational cost and renewable integration, compared to centralized decision-making; however, these losses can be greatly mitigated by having ERN and PDN operators share information about the planned EV charging demand and the projected locational marginal electricity price.

## 1. Introduction

Electric vehicles (EVs) are increasingly deployed worldwide (International Energy Agency (IEA), 2020), due to their potential contribution to reducing green house gas emissions, increased economic viability and convenience for the users. However, this brings new challenges to both the transportation and power systems. EV drivers need to consider the charging cost and time at different charging stations, when planning their trips. Traffic patterns are affected by the electricity price and the locations of fast charging stations (FCSs). On the one hand, the spatial and temporal charging demand resulting from the EVs charging patterns impacts the distribution of power flow, which challenges the operation of the existing power systems. On the other hand, this provides opportunities to efficiently operate power systems through vehicle-to-grid exchanges which could stabilize the power flow under the conditions of increased integration of renewable energy. In this setting, the power systems and the electrified road networks (ERNs) interact with each other through the dynamics of electricity price and charging demand. Such interplay brings challenges to control and operate the two systems, but also brings opportunities to promote integration and communication between each other.

Investigating how to model, operate and control the coupled ERNs and power systems considering EV charging has gained attention in recent years (Chen & Deng, 2024; Ding, Teng, Sarikprueck, & Hu, 2020; Teng, Ding, Hu, & Sarikprueck, 2020; Zheng, Niu, Shang, Shao, & Jian, 2019). Some of the main challenges addressed in the literature are how to properly model the physical features of the coupled transportation systems and power systems, as well as, modeling EVs and EVs supply equipment.

Some studies only consider the ERNs, ignoring the technical constraints coming from the power systems. Their objectives are mainly of optimizing allocation of FCSs (Bai et al., 2022; Chen, Qian, Miao, & Ukkusuri, 2020; Kchaou-Boujelben & Gicquel, 2020; Liu, Zou, Chen, & Long, 2021; Vosooghi, Puchinger, Bischoff, Jankovic, & Vouillon, 2020; Yazdekhasti, Jazi, & Ma, 2021), charging navigation

* Corresponding author.
*E-mail address:* yiping.fang@centralesupelec.fr (Y.-P. Fang).

https://doi.org/10.1016/j.cie.2024.110474
Received 21 December 2023; Received in revised form 19 June 2024; Accepted 9 August 2024
Available online 22 August 2024

## Nomenclature

### Indices

| | |
|---|---|
| $a$ | index of links |
| $t$ | index of periods |
| $s$ | index of destinations |
| $c$ | index for classes of EVs |
| $e$ | index for energy levels of EVs |

### The electrified road network sets

| | |
|---|---|
| $\mathcal{A}$ | set of arcs |
| $\mathcal{N}$ | set of nodes |
| $A(i)$ $(B(i))$ | set of links whose tail (head) node is $i$ |
| $\mathcal{A}_R$ | set of source arcs |
| $\mathcal{A}_S$ | set of sink arcs |
| $\mathcal{A}_G$ | set of general arcs |
| $\mathcal{A}_C$ | set of charging arcs |
| $\mathcal{T}$ | set of periods |

### Parameters

| | |
|---|---|
| $\phi$ | time value |
| $p_a^{ev}$ | charging power of charging link $a$ |
| $NC_a(t)$ | number of chargers at charging link $a$ during period $t$ |
| $\delta$ | period length |
| $L_a$ | physical length of link $a$ |
| $k_{jam}/q_{max}/v_f$ | jam density/ maximum flow/ free-flow speed |
| $w$ | backward shock-wave speed, $w = q_{max} \cdot v_f/(q_{max} - k_{jam} \cdot v_f)$ |
| $\alpha_a^t$ | average charging speed for charging link $a$ during period $t$, $\alpha_a^t = p_a^{ev}/(\eta \cdot v_f)$ |
| $f_a^I(t)$ | inflow capacity of link $a$ during period $t$ |
| $f_a^O(t)$ | outflow capacity of link $a$ during period $t$ |
| $DG_a^s(t)$ | cumulative gasoline vehicle travel demand between the entry of origin link $a$ and destination $s$ at the end of period $t$ |
| $\nu_a$ | free-flow travel time on link $a$, $\nu_a = L_a/(\delta \cdot v_f)$ |
| $\beta_a$ | travel time required by the backward shock wave from the exit to the entry of link $a$, $\beta_a = L_a/(\delta \cdot w)$ |

### Variables

| | |
|---|---|
| $U_a(t)$ | cumulative number of vehicles that enter link $a$ by the end of period $t$ |
| $V_a(t)$ | cumulative number of vehicles that leave link $a$ by the end of period $t$ |
| $UG_a(t)$ | cumulative number of GVs that enter link $a$ by the end of interval $t$ |
| $UG_a^s(t)$ | cumulative number of GVs that enter link $a$ to destination $s$ by the end of period $t$ |
| $VG_a(t)$ | cumulative number of GVs that leave link $a$ by the end of interval $t$ |
| $VG_a^s(t)$ | cumulative number of GVs that leave link $a$ to destination $s$ by the end of period $t$ |
| $UE_{a,c}^{s,e}(t)$ | cumulative number of EVs of class $c$ with energy level $e$ that enter link $a$ to destination $s$ by the end of period $t$ |
| $VE_{a,c}^{s,e}(t)$ | cumulative number of EVs of class $c$ with energy level $e$ that leave link $a$ to destination $s$ by the end of period $t$ |
| $x_{a,c}^{s,e}(t)$ | occupancy of EVs of class $c$ with energy level $e$ at charging link $a$ during period $t$ |
| $\hat{x}_{a,c}^{s,e}(t)$ | occupancy of EVs of class $c$ with the **updated** energy level $e$ at charging link $a$ during period $t$ |

### The electric vehicle sets

| | |
|---|---|
| $C$ | set of electric vehicle classes |

### Parameters

| | |
|---|---|
| $B_c$ | battery capacity of EVs of class $c$ |
| $E_c$ | maximum energy level of the EVs of class $c$ |
| $\eta$ | energy consumption of EVs |
| $\rho_a$ | energy levels required to traverse link $a$, $\rho_a = L_a/\eta$ |
| $L_c^{max}$ | driving range of EVs of class $c$, $L_c^{max} = B_c/\eta$ |
| $\mathcal{E}_c$ | set of energy levels for the EVs belonging to class $c$, $\mathcal{E}_c = L_c^{max}/(\delta \cdot v_f)$ |

### The power network sets

| | |
|---|---|
| $\mathcal{P}_N$ | set of buses |
| $\mathcal{P}_L$ | set of distribution lines |
| $\Gamma(j)$ | Successor set of bus $j$ |

### Parameters

| | |
|---|---|
| $a_j, b_j$ | Energy production cost coefficients at bus $j$ |
| $\mu(t)$ | Contract electricity price with the main grid in period $t$ |
| $p_j^{ramp}$ | Ramp limits of generators at bus $j$ |

### Variables

| | |
|---|---|
| $p_j^g(t)$ | Active power generation at bus $j$ during period $t$ |
| $p_j^{dc}(t)$ | Charging load at bus $j$ during period $t$ |
| $P_{ij}(t)$ | Active/Reactive power flowing from buses $i$ to $j$ during period $t$ |

### Acronym

| | |
|---|---|
| EVs | Electric Vehicles |
| FCSs | Fast Charging Stations |
| ERN | Electrified Road Network |
| PDN | Power Distribution Network |

(Erdoğan, Tural, & Khoei, 2023; Qian, Shao, Wang, & Shahidehpour, 2019) and routing (Alqahtani, Scott, & Hu, 2022; Basso, Kulcsár, Sanchez-Diaz, & Qu, 2022; Hiermann, Hartl, Puchinger, & Vidal, 2019; Tahami, Rabadi, & Haouari, 2020; Zhang et al., 2022), as well as simulating coordinated and uncoordinated charging modes (Zhang, Wang, & Qu, 2021). Some studies, instead, only consider detailed power systems modeling including EVs charging load, without considering realistic features of ERNs. Some of the topics considered can be summarized as: (1) Investigating the impacts of EVs on power systems in terms of safety (Wang, Dehghanian, Wang, & Mitolo, 2019), reliability (Hariri, Hejazi, & Hashemi-Dezaki, 2021; Li, Zhao, Zhang, Ye, & He, 2024), normal operation (Tang & Wang, 2016), among others. (2) Long-term planning problems (Quddus, Kabli, & Marufuzzaman, 2019), e.g., optimizing the allocation of smart grid components and charging stations (Tran, Keyvan-Ekbatani, Ngoduy, & Watling, 2021);

reinforcing power systems capacity to enable the massive deployment of solar photovoltaics, electric heat pumps and EVs, among others. (3) Coordinating EVs charging (He, Liu, & Song, 2020), such as, minimizing the number of coordinated EVs to mitigate voltage unbalance (Islam, Lu, Hossain, & Li, 2020); coordinating EVs charging while maintaining the voltage deviation within acceptable power quality limits (Zahedmanesh, Muttaqi, & Sutanto, 2020); managing day-ahead electricity procurement and real-time EVs charging to minimize the total operating cost (Liu et al., 2018). In the majority of cases, the spatial and temporal charging demand are required to be estimated statistically from existing data, which is, however difficult to access.

Other studies consider the coupled power systems and ERNs, and investigate the interdependency between the two systems. The literature presents traffic-power models typically comprising three components: a dynamic traffic assignment (DTA) model or a static traffic assignment (STA) model, an electric power model, and interdependent/dependent mechanisms. Several frameworks (Shin, Choi, & Kim, 2019; Wang, Fang, & Zio, 2021; Yang, Guo, Xu, & Sun, 2021) have been proposed to capture the interaction of traffic-power systems, with most models incorporating electricity price, EV charging or discharging behaviors, and traffic tolls to regulate the coupled systems. However, understanding the precise nature of interactions between these coupled systems remains an open issue. In modeling the electric power system, alternating current (AC) (Lv, Wei, Chen, Sun, & Wang, 2021; Xie, Xu, & Zheng, 2021) or direct current (DC) (Wei, Tang, & Hong, 2021; Yan, Zhao, & Guan, 2024; Zhao, Yan, Liu, & Ding, 2022) power flow models are commonly utilized. DTA models consist of a route choice model (i.e., assignment mechanism) and a dynamic network loading (DNL) model for propagating traffic flow through assigned routes in the network. System optimal (SO) and dynamic user equilibrium (DUE) assignment are two typical traffic assignment principles in the context of dynamic traffic-power models. Exit functions (Xie et al., 2021), link performance functions (Lv et al., 2021), and discrete versions of the continuum kinematic wave model (e.g., cell transmission models (Wei et al., 2021) and link transmission models (Yan et al., 2024)) are three main approaches for describing traffic flow propagation within an analytical DTA framework in relation to traffic-power dynamics. How to accommodate the critical characteristics related to EVs and charging infrastructures into traditional DTA models is a primary concern in the existing literature.

In this paper, we consider that the traffic flow within the ERNs and the power flow are interdependent through the charging demand at each FCS and the associated locational marginal price (LMP). Within this interaction process, from an ERN operator's perspective, the dynamic electricity price (i.e., LMP) and the capacity of FCSs are important parameters. The former is obtained from power systems and the latter is a key physical feature of an ERN. Both can influence the route choice of EV drivers and non-EV drivers, since EV drivers share the limited capacity of an FCS, and EVs and non-EV drivers share the limited capacities of roads. Therefore, traffic flow patterns are affected by both factors and, further impact the distribution of charging demand. From a power system operator's perspective, the accurate data of the spatial and temporal charging demand from an ERN can help to manage electricity production and balance the power flow of the systems. The spatial and temporal charging loads affect the power flow distribution subject to power system constraints, such as limitation of the grid and generator capacities, as well as ramp limits of generators. The power flow distribution, in return, influences the LMP, which would further affect traffic flow distribution. In this way, the ERN and power system interact with each other and both FCSs and EVs play critical roles in these interdependent traffic-power systems. The former is the interface connecting the ERN and power system, and the latter acts as the power prompting the interplay between traffic and power flow. Therefore, properly modeling the detailed physical features of EVs and FCSs is important to adequately study the interaction between the ERN and the power system. Here, we list some of the critical features that need to be modeled when investigating the interdependency of traffic-power systems and how they have been considered in the literature. A detailed comparison of these features in the literature is listed in Table 1.

**Dynamics** (feature of the coupled systems): A dynamic traffic-power system model is required due to: (1) the spatial and temporal nature of EVs; (2) the time-varying evolution of traffic flow; (3) the ramp limits of power generators. Most existing studies only considered a static model (Geng et al., 2019; Wang, Shahidehpour, Jiang, & Li, 2018; Wei, Wu, Wang, & Mei, 2018; Zhang, Hu, & Song, 2020), whereas recently increasing attention has been paid to modeling dynamic (Rossi, Iglesias, Alizadeh, & Pavone, 2019; Zhou, Zhang, Guo, & Sun, 2021) or semi-dynamic (Lv, Wei, Sun, Chen, & Zang, 2019) traffic-power systems.

**Charging time** (feature of EV): It is part of the travel time cost, when the time value is considered. Refs. Geng et al. (2019), Xie, Hu, Wang, and Chen (2020) assumed that all EVs, had (A1) the same exogenously given fixed charging time. This assumption is marked as (A1).

**Charging demand** (feature of EV): It influences the charging cost for EV drivers, and influences power production as well as power flow distribution. Refs. Geng et al. (2019), Wang et al. (2018), Wei et al. (2018), Xie et al. (2020) assumed all EVs had (A2) the same exogenously given fixed charging demand; Refs. Lv et al. (2019), Wang et al. (2018), Zhou et al. (2021) assumed the charging demand was (A3) only related to traffic flow through the FCSs without considering the real charging needs. It could cause the EVs to charge multiple times without considering the remaining battery capacity leading to an overestimation of the charging demand.

**Driving range/Battery capacity** (feature of EV): It influences the number of times an EV has to recharge during a trip.

**Initial state of charge (SoC)** (feature of EV): It influences whether it is required to recharge an EV at the beginning of the time horizon. If it has, the initial SoC of an EV influences which FCSs this EV is able to reach without running out of battery. Ref. Wei et al. (2018) assumed (A4) an EV was able to reach any FCS. This assumption may result in the assigned charging point being beyond the remaining driving range of an EV.

**Mix of gasoline vehicles (GVs)** (feature of an ERN): EVs and GVs compete for the limited road capacity.

**Capacity of FCSs** (feature of an ERN): EVs compete for the limited charging capacities at FCSs.

Additionally, several decision-making environments considered for co-operations of traffic-power systems are summarized in Table 1. *Centralized* decision-making environments describe a situation where there is a single operator who controls both ERNs and power systems in a fully integrated manner. Their objectives usually lead to a social optimum. *Decentralized* decision-making environments describe a situation where ERNs and power systems operate independently, but they can share their operation plans at the beginning of each time step (Zhou et al., 2021) or at the beginning of the time horizon (Geng et al., 2019; Rossi et al., 2019; Wei et al., 2018). Their own plans are not necessarily changed according to the received information. They also can exchange their plans for any number of rounds. The decentralized situation in Table 1 assumed that both the ERN operator and the power system operator share their information until converging (e.g., the changes of traffic flow pattern and charging price are smaller than a threshold (Wei et al., 2018)) or meeting the maximum iteration rounds. Refs. Geng et al. (2019), Wei et al. (2018), Zhou et al. (2021) showed that, under a sufficient information-sharing situation, the solution approximates an equilibrium between ERNs and power systems. Furthermore, Ref. Rossi et al. (2019) has proved that the social optimum is a general equilibrium if LMP is used in power systems, where the power system operator is a nonprofit one whose objective is to balance the electricity supply and demand under technical security constraints. Since the power system operator is welfare-minded, it can steer a selfish ERN operator toward the social optimum. More discussions are detailed in Refs. Rossi

**Table 1**
Summary of considered factors in relevant literature.

| References | Decision-making environments | Dynamics | EV features | | | | ERNs features | |
|---|---|---|---|---|---|---|---|---|
| | | | Charging time | Charging demand | Driving range | Initial SoC | GVs | Capacityof FCSs |
| Xie et al. (2021) | decentralized | ✓ | (A1) | (A2) | × | × | ✓ | ✓ |
| Lv et al. (2021) | decentralized | ✓ | (A1) | (A3) | × | × | ✓ | × |
| Yan et al. (2024) | decentralized | ✓ | (A1) | ✓ | ✓ | ✓ | ✓ | × |
| Wei et al. (2021) | decentralized | ✓ | × | (A3) | × | × | ✓ | × |
| Sun et al. (2020) | centralized | ✓ | (A1) | (A2) | × | × | × | ✓ |
| Zhou et al. (2021) | decentralized | ✓ | × | (A3) | × | × | × | ✓ |
| Sun et al. (2020) | centralized | ✓ | (A1) | (A2) | × | × | × | ✓ |
| Lv et al. (2019) | centralized | ✓ | × | (A3) | × | × | × | × |
| Zhang et al. (2020) | centralized | × | ✓ | ✓ | ✓ | ✓ | × | × |
| Wei et al. (2018) | decentralized | × | ✓ | (A2) | × | (A4) | ✓ | ✓ |
| Wang et al. (2018) | centralized | × | × | (A3) | ✓ | ✓ | × | ✓ |
| Geng et al. (2019) | decentralized | × | (A1) | (A2) | × | × | ✓ | ✓ |
| Xie et al. (2020) | centralized | × | (A1) | (A2) | × | × | ✓ | ✓ |
| Xie et al. (2020) | centralized | × | (A1) | (A2) | × | × | ✓ | ✓ |

et al. (2019). Ref. Wang, Fang, and Zio (2022) briefly discussed the impact of EVs on the independent and interdependent traffic-power systems from a disruptive event, however, it mainly focused on modeling reconfiguration strategies from the system's topological perspective to optimize the restoration planning for traffic-power systems. Different from Ref. Wang et al. (2022), this paper concentrates on investigating the coordinating dynamic traffic-power systems under decentralized and centralized decision-making environments. Consequently, the main tasks of this paper are to build the mathematical formulations of the decision-making environments and propose the corresponding solving algorithm. To sum up, a systematic analysis of the interaction of traffic-power systems under different decision-making environments is missing, as shown in Table 1.

To fill the research gaps mentioned above, this paper proposes a dynamic traffic-power system model and investigates the coordination of traffic-power systems under centralized and decentralized decision-making environments.

The main contributions of the paper are summarized as follows:

(1) We propose a novel dynamic traffic-power system model, which is able to capture the spatial–temporal traffic flow evolution and charging demand. Dynamic models can provide more accurate charging load information compared to static ones. Within the proposed model, the critical features of EVs and ERNs, summarized in Table 1, are thoroughly considered. Moreover, the proposed model also considers the different classes of EVs with different driving ranges, chargers with different charging powers in an FCS and the charging process of EVs. These extensions allow the model to be used in various applications and at different granularities.

(2) This paper systematically investigates the operation of traffic-power systems under centralized and decentralized decision-making environments. The corresponding mathematical models under different decision-making environments are formulated.

(3) An iterative algorithm is proposed to solve the centralized optimization problem. We compare the decision-making environments in terms of the charging congestion level at FCSs, charging price, charging demand, and integration of renewable energy, among others.

The remainder of the article is structured as follows. Section 2 develops the traffic-power system model. Section 3 describes decentralized and centralized decision-making environments. Section 4 illustrates a numerical example to show the application of the proposed model and compare the solutions under different decision-making environments. Finally, Section 5 provides some concluding remarks and future research directions.

## 2. Coupled traffic-power system

### 2.1. Link transmission model based system optimal dynamic traffic assignment problem

In the link transmission model (LTM) (Long & Szeto, 2019; Yperman, 2007), a triangular fundamental diagram serves as an approximation to describe the macroscopic features of roads, considering various factors such as the number of lanes, weather conditions, and speed limits (Yperman, 2007). This diagram is characterized by three primary parameters: a jam density ($k_{jam}$), a maximum flow ($q_{max}$), and a fixed-free flow speed ($v_f$). The backward shock-wave speed $w$ can be calculated using the formula $w = q_{max} \cdot v_f/(q_{max} - k_{jam} \cdot v_f)$. Within the LTM framework, the progression of traffic flow is updated by computing the cumulative count of vehicles at both the entry and exit points of each link during specific time intervals. The time frame $H$ is partitioned into a finite series of intervals $\mathcal{T} = t = 1, 2, \ldots, T$. The determination of $T$ employs the formula $T = H/\delta$, where $\delta$ indicates the duration of each interval. This interval duration must either match or be smaller than the minimum travel time of the links, ensuring that vehicles necessitate at least one unit of time to traverse a link (Yperman, 2007).

The representation of a roadway network featuring multiple origins and destinations is symbolized as $G(\mathcal{N}, \mathcal{A})$, where $\mathcal{N}$ and $\mathcal{A}$ stand for the collections of nodes and links. The entirety of links and nodes within this network is sorted into three distinct classifications: origins, destinations, and general nodes or links. Within this network framework, each origin (destination) node exclusively pairs with an (a) origin (destination) link. Identified by $\mathcal{N}_R$ (alternatively $\mathcal{N}_S$) and $\mathcal{A}_R$ ($\mathcal{A}_S$), these sets specifically demarcate the nodes linked with origins (destinations) and the links connected to origins (destinations). Links indicated as origins or destinations are artificially created links, characterized by a length of zero and possessing infinite outflow, inflow, and storage capacities. Concerning the System Optimal Dynamic Traffic Assignment (SO-DTA) problem, the presumption is that the outflow capacity of all destination links is zero, indicating the accumulation of all vehicles upon their arrival.

The limitations on the inflow and outflow of link $a$ within interval $t$ are governed by the subsequent equations, which is derived from Newell (1993a, 1993b):

$$U_a(t) - U_a(t-1) \leq \min V_a(t - \beta_a) + L_a \cdot k_{jam} - U_a(t-1), f_a^I(t), \forall a \in \mathcal{A}, t \in \mathcal{T} \tag{1a}$$

$$V_a(t) - V_a(t-1) \leq \min U_a(t - v_a) - V_a(t-1), f_a^O(t), \forall a \in \mathcal{A}, t \in \mathcal{T} \tag{1b}$$

In Eq. (1), the left-hand term symbolizes the inflow (outflow) of link $a$ during interval $t$, while the right-hand term corresponds to its receiving (sending) capacities. $U_a(t)$ ($V_a(t)$) represents the cumulative count of vehicles that enter (exit) link $a$ by the end of interval $t$, respectively. Additionally, $f_a^I(t)$ and $f_a^O(t)$ denote the inflow capacity at the entry point and outflow capacity at the exit point of link $a$ throughout period $t$. These capacities are determined by $\delta \cdot q_{max}$ at the respective location and time. Furthermore, $L_a$ denotes the length of link $a$, $\nu_a$ indicates the free-flow travel duration on link $a$, and $\beta_a$ denotes the time taken by the backward shock wave from the departure to the arrival of link $a$. Their values are calculated as $\nu_a = L_a/(\delta \cdot v_f)$ and $\beta_a = L_a/(\delta \cdot w)$, respectively.

In the LTM-based SO-DTA problem, the different classes of vehicles are not distinguished. Thus, we have:

$$U_a(t) = \sum_{s\in\mathcal{N}_S} UG_a^s(t), \forall a \in \mathcal{A}, t \in \mathcal{T} \tag{2a}$$

$$V_a(t) = \sum_{s\in\mathcal{N}_S} VG_a^s(t), \forall a \in \mathcal{A}, t \in \mathcal{T} \tag{2b}$$

where $UG_a^s(t)(VG_a^s(t))$ denotes the cumulative number of gasoline vehicles that enter(leave) link $a$ to destination $s$ by the end of period $t$.

Substituting Eq. (2) into the inequalities in Eq. (1), the linear LTM-based flow constraints are obtained as follows:

$$\sum_{s\in\mathcal{N}_S} VG_a^s(t) \le \sum_{s\in\mathcal{N}_S} UG_a^s(t-\nu_a), \forall a \in \mathcal{A}, t \in \mathcal{T} \tag{3}$$

$$\sum_{s\in\mathcal{N}_S} [VG_a^s(t) - VG_a^s(t-1)] \le f_a^O(t), \forall a \in \mathcal{A}, t \in \mathcal{T} \tag{4}$$

$$\sum_{s\in\mathcal{N}_S} UG_a^s(t) \le \sum_{s\in\mathcal{N}_S} VG_a^s(t-\beta_a) + L_a \cdot k_{jam}, \forall a \in \mathcal{A}, t \in \mathcal{T} \tag{5}$$

$$\sum_{s\in\mathcal{N}_S} [UG_a^s(t) - UG_a^s(t-1)] \le f_a^I(t), \forall a \in \mathcal{A}, t \in \mathcal{T} \tag{6}$$

The cumulative outflow to destination $s$ should be constrained by the cumulative inflow to the same destination on link $a$:

$$VG_a^s(t) \le UG_a^s(t-\nu_a), \forall a \in \mathcal{A}, t \in \mathcal{T} \tag{7}$$

The fulfillment of the traffic demand is achieved by ensuring that the total inflow from the source links equals the cumulative demands.

$$UG_a^s(t) = DG_a^s(t), \forall a \in \mathcal{A}_R, \forall s \in \mathcal{N}_S, t \in \mathcal{T} \tag{8}$$

where $DG_a^s(t)$ denotes the cumulative travel demand for gasoline-vehicles originating from link $a$ and heading towards destination $s$ by the conclusion of period $t$.

Within the LTM model, flow conservation constraints must limit both the incoming and outgoing traffic flows of a general node in the following manner:

$$\sum_{a\in B(i)} VG_a^s(t) = \sum_{a\in A_{(i)}} UG_a^s(t), \forall i \in \mathcal{N}/\{\mathcal{N}_R, \mathcal{N}_S\}, \forall s \in \mathcal{N}_S, t \in \mathcal{T} \tag{9}$$

where $A(i)$ denotes the collection of links with their starting node as $i$, while $B(i)$ signifies the set of links where $i$ serves as their terminal node.

The cumulative flows are required to be both non-negative and non-decreasing:

$$VG_a^s(t) - VG_a^s(t-1) \ge 0, \forall a \in \mathcal{A}, \forall s \in \mathcal{N}_S, t \in \mathcal{T} \tag{10}$$

$$UG_a^s(t) - UG_a^s(t-1) \ge 0, \forall a \in \mathcal{A}, \forall s \in \mathcal{N}_S, t \in \mathcal{T} \tag{11}$$

The subsequent equations enforce that the initial cumulative flows start from zero:

$$UG_a^s(0) = VG_a^s(0) = 0, \forall a \in \mathcal{A}, \forall s \in \mathcal{N}_S \tag{12}$$

The objective of the SO-DTA problem based on LTM is to minimize the collective travel duration for all vehicles, computed as the cumulative time vehicles spend on all links throughout the entire time span. The LTM-based SO-DTA problem (Long & Szeto, 2019) is formulated as follows:

$$\min_{x\in\Omega} \sum_{a\in\mathcal{A}/\mathcal{A}_S} \sum_{s\in\mathcal{N}_S} \sum_{t\in\mathcal{T}} \delta[UG_a^s(t) - VG_a^s(t)] \tag{13}$$

where $\boldsymbol{x} = \{\boldsymbol{UG}, \boldsymbol{VG}\}$ and $\Omega = \{\boldsymbol{x} |$ s.t. (3)–(12)$\}$.

### 2.2. eLTM-based SO-DTA problem

For completeness, the electric link transmission model (Wang et al., 2022) is illustrated here. Ref. Wang et al. (2022) focused on modeling reconfiguration strategies from the system's topological perspective to optimize the restoration planning for traffic-power systems. However, this paper concentrates on investigating the coordinating dynamic traffic-power systems under decentralized and centralized decision-making environments.

The existing LTM-based SO-DTA model is not able to describe the new features related to the EVs, such as the driving range of EVs and the capacity of FCSs, an eLTM-based SO-DTA model (Wang et al., 2022) is adopted to minimize the total cost for all vehicles considering the EVs driving ranges, FCS capacities, charging costs, among others.

The assumptions in this model are:

(1) An EV charges the minimum en-route to ensure the shortest travel time. The SoC after charging (original SoC plus the charged electricity) should ensure that the EV can reach the destination or the next FCS. This assumption is coherent with the objective function of the proposed model, which is to minimize the total cost. As for the heterogeneous charging preferences of EV drivers, their consideration is not within the scope of this paper.

(2) An EV's energy consumption correlates linearly with the distance covered, as shown in Refs. Bi, Wang, and Zhang (2018), Dunckley (2018) based on empirical data analysis.

(3) EV drivers charge their batteries between 20%–80% of SoC, and the amount of electricity charged in an EV is linearly related to the charging duration (Kostopoulos, Spyropoulos, & Kaldellis, 2020; Patnaik, Praneeth, & Williamson, 2018; Wang, Liu, Du, & Kong, 2016; Yang, Zhang, Ge, & Wang, 2018). This assumption takes into consideration factors such as EV range anxiety, minimizing travel time, and protecting the Li-ion battery from over-discharge and overcharge.

(4) All EV batteries exhibit an identical energy consumption efficiency, as discussed in Ref. He, Yin, and Lawphongpanich (2014).

(5) The electricity usage of in-vehicle utilities like air conditioning and lighting is disregarded. When EVs are stationary, there is no electricity consumption.

In order to track the SoC of EVs, the model accounts for different energy levels to describe the real-time SoC for each EV. Given a certain class of EV denoted as $c$, the mileage of this class EV is given by $L_c^{max}$ miles. An Energy Level (EL) is defined as $\delta \cdot v_f$ miles. Hence, the maximum EL for an EV of class $c$ is calculated as $E_c = L_c^{max}/(\delta \cdot v_f)$. If there are $C$ EV classes denoted as $\mathcal{C} = \{\mathcal{E}_1, \mathcal{E}_2, \dots, \mathcal{E}_C\}$, each element within set $\mathcal{C}$ constitutes a set. These sets, denoted as $\mathcal{E}_c = \{1, 2, \dots, E_c\}$, represent the various energy levels achievable by EVs in class $c$.

In the initial formulation of the eLTM-based model (Wang et al., 2022), dummy charging links $\mathcal{A}_C$ were introduced to indicate the Fast Charging Stations (FCSs) within the physical ERN. These FCSs are represented by one or multiple charging links, depicted as arcs sharing identical origin and destination points. Each charging link symbolizes chargers of varied charging speeds. The parameter $\alpha_a^t$ denotes the average charging speed attributed to charging link $a$ during period $t$. It quantifies the number of energy levels deliverable by a type $a$ charger within a period $\delta$, reflecting the charging speed in terms of energy levels supplied per unit time. The lengths of charging links are considered to be 0. For every charging link $a$, $NC_a(t)$ is specified as the actual count

of chargers of type $a$ during time period $t$. Typically, both the charging speed $\alpha_a^t$ and the charger count $NC_a(t)$ remain constant.

Given a general link $a$, its length is $L_a$; then, the consumed ELs on link $a$ is calculated by $\rho_a = L_a/(\delta \cdot v_f)$. $UE_{a,c}^{s,e}(t)$ (or $VE_{a,c}^{s,e}(t)$) represents the accumulated count of EVs categorized as type $c$ with energy level $e$, which either enter (for $UE$) or leave (for $VE$) link $a$ heading towards destination $s$ during period $t$.

Based on the inequalities in Eq. (1), the mixed flow constraints for EVs and conventional vehicles in the eLTM-based model are derived in the following manner:

$$VE_{a,c}^{s,e}(t) \le UE_{a,c}^{s,e+\rho_a}(t-\nu_a), \forall a \in \mathcal{A}\backslash\{\mathcal{A}_C\}, \forall s \in \mathcal{N}_S, \forall c \in C, e \in \mathcal{E}_c \cap \{e \le E_c - \rho_a\}, t \in \mathcal{T} \tag{14a}$$

$$VE_{a,c}^{s,e}(t) = 0, \forall a \in \mathcal{A}\backslash\{\mathcal{A}_C\}, \forall s \in \mathcal{N}_S, \forall c \in C, e \in \mathcal{E}_c \cap \{e > E_c - \rho_a\}, t \in \mathcal{T} \tag{14b}$$

$$\sum_{s\in\mathcal{N}_S}[VG_a^s(t) - VG_a^s(t-1)] + \sum_{s\in\mathcal{N}_S}\sum_{c\in C}\sum_{e\in\mathcal{E}_c}[VE_{a,c}^{s,e}(t) - VE_{a,c}^{s,e}(t-1)] \le Of_a(t), \forall a \in \mathcal{A}\backslash\{\mathcal{A}_C\}, t \in \mathcal{T} \tag{15}$$

$$\sum_{s\in\mathcal{N}_S}\sum_{c\in C}\sum_{e\in\mathcal{E}_c}[UE_{a,c}^{s,e}(t) - VE_{a,c}^{s,e}(t-\beta_a)] + \sum_{s\in\mathcal{N}_S}[UG_a^s(t) - VG_a^s(t-\beta_a)] \le L_a k_{jam}, \forall a \in \mathcal{A}\backslash\{\mathcal{A}_C\}, t \in \mathcal{T} \tag{16}$$

$$\sum_{s\in\mathcal{N}_S}[UG_a^s(t) - UG_a^s(t-1)] + \sum_{s\in\mathcal{N}_S}\sum_{c\in C}\sum_{e\in\mathcal{E}_c}[UE_a^s(t) - UE_a^s(t-1)] \le If_a(t), \forall a \in \mathcal{A}\backslash\{\mathcal{A}_C\}, t \in \mathcal{T} \tag{17}$$

Eq. (14a) ensures that the outflow is constrained to be less than or equal to the inflow, with the deducted ELs occurring after the EVs have traversed the corresponding links. Eq. (14b) guarantees that the ELs of EVs remain below their maximum ELs. Eqs. (15) to (17) mirror the counterparts in Eqs. (4) to (6). Both (15) and (17) constrain the outflow and inflow to be less than or equal to their respective capacities, while Eq. (16) guarantees that the count of vehicles on link $a$ must not exceed the maximum capacity of vehicles that can be accommodated on this link.

Eq. (18) ensures that the traffic demand of EVs should also be satisfied:

$$UE_{a,c}^{s,e}(t) = DE_{a,c}^{s,e}(t), \forall a \in \mathcal{A}_R, \forall s \in \mathcal{N}_S, \forall c \in C, \forall e \in \mathcal{E}_c, t \in \mathcal{T} \tag{18}$$

Similar to Eq. (9), the EV flows also obey the flow conservation law, formulated as follows:

$$\sum_{a\in B(i)} VE_{a,c}^{s,e}(t) = \sum_{a\in A_{(i)}} UE_{a,c}^{s,e}(t), \forall i \in \mathcal{N}/\{\mathcal{N}_R, \mathcal{N}_S\}, \forall s \in \mathcal{N}_S, \forall c \in C, \forall e \in \mathcal{E}_c, t \in \mathcal{T} \tag{19}$$

### 2.2.1. Modeling EV charging process

To model the charging process, intermediate variables $\hat{x}_{a,s}^{s,e}(t)$ and $x_{a,s}^{s,e}(t)$ are defined as the number of EVs before and after their ELs have been updated on charging link $a$. The occupancy $\hat{x}_{a,s}^{s,e}(t)$ on a charging link is calculated by the occupancy plus new inflow minus outflow during the previous period, as shown in Eq. (20):

$$\hat{x}_{a,s}^{s,e}(t) = x_{a,s}^{s,e}(t-1) + [UE_{a,c}^{s,e}(t-1) - UE_{a,c}^{s,e}(t-2)] - [VE_{a,c}^{s,e}(t-1) - VE_{a,c}^{s,e}(t-2)], \forall a \in \mathcal{A}_C, \forall s \in \mathcal{N}_S, \forall c \in C, \forall e \in \mathcal{E}_c, t \in \mathcal{T} \tag{20}$$

Furthermore, the following equations describe the process of updating the ELs on charging links:

$$x_{a,c}^{s,E_c}(t) = \sum_{l=0}^{\alpha_a^t} \hat{x}_{a,c}^{s,E_c-l}(t), \ \forall a \in \mathcal{A}_C, \forall s \in \mathcal{N}_S, \forall c \in C, \forall t \in \mathcal{T} \tag{21a}$$

$$x_{a,c}^{s,e}(t) = \hat{x}_{a,c}^{s,e-\alpha_a^t}(t), \ \forall a \in \mathcal{A}_C, \forall s \in \mathcal{N}_S, \forall c \in C, \forall e \in \{\alpha_a^t \le e < E_c\}, \forall t \in \mathcal{T} \tag{21b}$$

$$x_{a,c}^{s,e}(t) = 0, \forall a \in \mathcal{A}_C, \forall s \in \mathcal{N}_S, \forall c \in C, \forall e \in \{e < \alpha_a^t\}, \forall t \in \mathcal{T} \tag{21c}$$

Eqs. (21a) and (21c) constrain the upper and lower bounds of the updated ELs. Eqs. (21b) describe the process of linear increase in ELs. Eq. (21a) states that if the ELs of EVs before being updated belong to $[E_c - \alpha_a^t, E_c]$, their energy levels are approximately updated as the maximum EL $E_c$ of EV of class $c$ after one period. Eq. (21b) states that if the ELs of EVs are within $[0, E_c - \alpha_a^t)$ before being updated, they increase $\alpha_a^t$ ELs after one period. The updated ELs are within $[\alpha_a^t \le e < E_c)$. Eq. (21c) ensures that no EVs' ELs are less than $\alpha_a^t$ level after being charged for one period. Therefore, if the updated ELs are smaller than $\alpha_a^t$, they are forced to be 0. Note that the number of EVs on charging links are conserved before and after the ELs of the EVs are updated, i.e., $\sum_e \hat{x}_{a,c}^{s,e}(t) = \sum_e x_{a,c}^{s,e}(t)$.

Furthermore, the outflow aggregated on EL along charging link $a$, does not exceed its occupancy, as expressed in Eq. (22):

$$VE_{a,c}^{s,e}(t) - VE_{a,c}^{s,e}(t-1) \le x_{a,c}^{s,e}(t), \forall a \in \mathcal{A}_C, \forall s \in \mathcal{N}_S, \forall c \in C, \forall e \in \mathcal{E}_c, \forall t \in \mathcal{T} \tag{22}$$

Eq. (23) limits the number of EVs on charging link $a$ to its maximum number of chargers:

$$\sum_{s\in\mathcal{N}_S}\sum_{c\in C}\sum_{e\in\mathcal{E}_c}[UE_{a,c}^{s,e}(t) - VE_{a,c}^{s,e}(t)] \le NC_a(t), \forall a \in \mathcal{A}_C, \forall t \in \mathcal{T} \tag{23}$$

Moreover, Eqs. (24)–(25) ensure that the cumulative EV flows are nonnegative and nondecreasing:

$$VE_{a,c}^{s,e}(t) - VE_{a,c}^{s,e}(t-1) \ge 0, \forall a \in \mathcal{A}, \forall s \in \mathcal{N}_S, \forall c \in C, \forall e \in \mathcal{E}_c, t \in \mathcal{T} \tag{24}$$

$$UE_{a,c}^{s,e}(t) - UE_{a,c}^{s,e}(t-1) \ge 0, \forall a \in \mathcal{A}, \forall s \in \mathcal{N}_S, \forall c \in C, \forall e \in \mathcal{E}_c, t \in \mathcal{T} \tag{25}$$

Similarly, the occupancies on charging links is nonnegative, as described in Eq. (26):

$$x_{a,c}^{s,e}(t) \ge 0, \ \hat{x}_{a,c}^{s,e}(t) \ge 0, \forall a \in \mathcal{A}_C, \forall s \in \mathcal{N}_S, \forall c \in C, \forall e \in \mathcal{E}_c, t \in \mathcal{T} \tag{26}$$

The occupancies on charging links and the cumulative EV flows are initialized to be 0, as formulated in Eq. (27):

$$UE_{a,c}^{s,e}(0) = VE_{a,c}^{s,e}(0) = 0, \forall a \in \mathcal{A}, \forall s \in \mathcal{N}_S, \forall c \in C, \forall e \in \mathcal{E}_c \tag{27}$$

As for the LTM-based SO-DTA problem, the objective of the eLTM-based SO-DTA problem is to minimize the total travel time, including the charging time of EVs. The problem is formulated as:

$$\min_{\boldsymbol{y}\in\Psi_T} \sum_{s\in\mathcal{N}_S}\sum_{t\in\mathcal{T}}\sum_{a\in\mathcal{A}/\{\mathcal{A}_C,\mathcal{A}_S\}} \delta[UG_a^s(t) - VG_a^s(t)] + \sum_{s\in\mathcal{N}_S}\sum_{t\in\mathcal{T}}\sum_{a\in\mathcal{A}/\mathcal{A}_S}\sum_{c\in C}\sum_{e\in\mathcal{E}_c} \delta[UE_{a,c}^{s,e}(t) - VE_{a,c}^{s,e}(t)] \tag{28}$$

where $\boldsymbol{y} = \{\boldsymbol{UG}, \boldsymbol{VG}, \boldsymbol{UE}, \boldsymbol{VE}\}$ and $\Psi_T = \{\boldsymbol{y} |$ s.t. (7)–(12) and (14)–(27)$\}$. It should be noted that for all $a$ in constraints (7)–(12) its domain does not include $\mathcal{A}_C$. It means conventional vehicles never go into charging links.

## 2.3. Power distribution network (PDN) model

We consider a radial PDN $\mathcal{G}_P(\mathcal{P}_N, \mathcal{P}_L)$, where $\mathcal{P}_N$ and $\mathcal{P}_L$ represent the sets of buses and distribution branches, respectively. In a radial network, each bus is attached to a unique predecessor bus and the number of buses equals that of branches, which excludes a slack bus. The slack bus is indexed as 0. The successor set of bus $j$ is denoted as $\Gamma(j) = \{\forall k : (j,k) \in \mathcal{P}_L\}$. The power system model in Ref. Wei et al. (2018) is employed in this paper. We additionally add constraint (29) to limit the generator ramp between two successive periods:

$$-p_j^{ramp} \le p_j^g(t) - p_j^g(t-1) \le p_j^{ramp}, \forall j \in \mathcal{P}_N, \forall t \in \mathcal{T} \tag{29}$$

where $p_j^g$ is the active power generation in period $t$ and $p_j^{ramp}$ is the ramp limits of generators at bus $j$.

The EV charging load in Ref. Wei et al. (2018) is calculated by the static traffic flow passing charging stations and the energy demand of each EV is assumed to be fixed. In our paper, the charging load during each period is calculated by the number of EVs stopping in charging links. The energy demand of each EV is consistent with the assumption (1) in Section 2.2. Thus, the EV charging load in Eq. (28) in Ref. Wei et al. (2018) is replaced by the following equation:

$$p_j^{dc}(t) = \sum_{a\in M(j)} \sum_{s\in\mathcal{N}_S} \sum_{c\in C} \sum_{e\in\mathcal{E}_c} p_a^{ev}[UE_{a,c}^{s,e}(t) - VE_{a,c}^{s,e}(t)] \tag{30}$$

where $M(j)$ is a mapping from bus set $\mathcal{P}_N$ to charging links set $\mathcal{A}_C$, which specifies the connection between buses in a power system and charging links in a road network. $N(a)$ is a reverse mapping of $M(j)$, which maps charging links set to the bus set. The LMP at each bus is denoted as $\lambda_j^t$. The charging price at charging link $a$ can be obtained by $\lambda_{N(a)}^t$.

To clearly describe the PDN model here, we detail the objective function used. The objective of the PDN operator is to minimize the total energy production costs. The optimal power flow problem is defined as **P1**:

$$\min_{z\in\Psi_P} \sum_{t\in\mathcal{T}} \sum_{j\in\mathcal{P}_N} [a_j(p_j^g(t))^2 + b_j p_j^g(t)] + \sum_{t\in\mathcal{T}} \sum_{k\in\Gamma(0)} \mu(t)P_{0k}(t) \tag{31}$$

$$\Psi_P = \{\boldsymbol{z}|\ \text{s.t. (29)–(30), and (24) – (34) in Ref. Wei et al. (2018)}\} \tag{32}$$

where $\boldsymbol{z} = \{\boldsymbol{p}^g, \boldsymbol{P}\}$; $a_j$ and $b_j$ are the production cost coefficients at bus $j$; $P_{0k}$ is the active power flow from main grid to bus $k$. The first term is the production cost of the local generators and the second term is the cost of purchasing electricity from the main grid. $\mu(t)$ is the contract energy price during period $t$ with the main grid.

## 3. Decision environments

In this section, two decision-making environments are considered for operating the traffic-power systems, which may arise when different beneficiaries coordinate the interdependent infrastructures. Analyzing different decision-making environments allows us to compare their operational and socially beneficial difference. The value of sharing information also can be studied.

### 3.1. Decentralized decision environments

In current practice, individual infrastructure systems such as ERNs and PDNs often determine their operation in an independent, decentralized manner. In this decision-making environment, the ERN operator minimizes the system operation cost. We adopt a system optimum model where the objective is to minimize the total travel cost through dynamic traffic assignment. The total travel cost includes the driving time cost of both EVs and GVs, the charging time cost of EVs and the charging cost of EVs. This optimal traffic flow problem **P2** is formulated as follows:

$$\begin{aligned}
&\min_{\boldsymbol{y}\in\Psi_T} \sum_{s\in\mathcal{N}_S} \sum_{t\in\mathcal{T}} \sum_{a\in\mathcal{A}/\{\mathcal{A}_C,\mathcal{A}_S\}} \phi\delta[UG_a^s(t) - VG_a^s(t)] \\
&+ \sum_{s\in\mathcal{N}_S} \sum_{t\in\mathcal{T}} \sum_{a\in\mathcal{A}/\mathcal{A}_S} \sum_{c\in C} \sum_{e\in\mathcal{E}_c} \phi\delta[UE_{a,c}^{s,e}(t) - VE_{a,c}^{s,e}(t)] + \\
&\sum_{s\in\mathcal{N}_S} \sum_{t\in\mathcal{T}} \sum_{c\in C} \sum_{e\in\mathcal{E}_c} \sum_{a\in\mathcal{A}_C} \lambda_{N(a)}^t p_a^{ev}\delta[UE_{a,c}^{s,e}(t) - VE_{a,c}^{s,e}(t)]
\end{aligned} \tag{33}$$

subject to constraints (7)–(12) and (14)–(27), where $\phi$ is the time value.

Considering the interaction between the ERN and the PN, whether information is exchanged or not between the two systems beforehand becomes important which usually makes operators' plans different. In our case, if the dynamic charging prices in FCS are known beforehand by the ERN operator, it will greatly influence the traffic assignment solution. Accordingly, the changed charging load distribution further makes the electricity production variation. To study the influence of information sharing, two benchmarks are studied in this paper: system operations make decisions with no information sharing and with information sharing.

#### 3.1.1. No information-sharing situation

In this situation, the ERN operator does not know the real-time electricity price $\lambda_{N(a)}^t$ beforehand, so we assume that an estimated fixed charging price is used for the operator. For the PDN, it is assumed that the operator only knows the real-time charging demand and the demand in the future time periods is unknown. Thus, **P1** is solved for each independent period for a total of $T$ times. The main process is shown in Fig. 1(a). At the beginning, the estimated charging price (LMP) for the ERN operator is used to solve **P1**. Then, in each period, the PDN operator receives the real-time charging demand from each FCS. Based on the real-time power demand, the operator solves **P2** to obtain the optimal power flow pattern $\boldsymbol{z}$ and the corresponding actual LMP in each period. Note that this price does not change the traffic assignment solutions. In the end, the actual charging cost for the ERN operator can be calculated by the actual LMP.

#### 3.1.2. Information-sharing situation

In this situation, the ERN operator and the PDN operator actively share (partial information about) their operation plans with each other, but do not necessarily fully coordinate or cooperate with each other. This situation assumes that the two operators exchange their expected plans at the beginning of the time horizon. Specifically, an ERN operator sends the expected charging demands information to the PDN operator. Based on the received information, the PDN operator calculates the expected electricity prices and communicates them to the ERN operator who updates its plan accordingly. This information-sharing behavior can be continued for any number of rounds and the number of rounds can be understood as time available for the operators to exchange information. The interplay process is shown in Fig. 1(b).

### 3.2. Centralized decision environments

The centralized decision-making environment assumes that there is a centralized operator that coordinates both the ERNs and the PDNs to minimize the total cost of the two systems. It means that ERNs and PDNs fully integrate with each other, although this may lead to sacrificing their own benefits from an independent system's perspective. This situation may be ideal, but the results can serve as a benchmark to understand and analyze the best possible coordination between ERNs and PDNs. This environment can be expressed as the following optimization problem:

$$\begin{aligned}
&\min_{\boldsymbol{w}\in\{\Psi_T\times\Psi_P\}} \sum_{s\in\mathcal{N}_S} \sum_{t\in\mathcal{T}} \sum_{a\in\mathcal{A}/\{\mathcal{A}_C,\mathcal{A}_S\}} \phi\delta[UG_a^s(t) - VG_a^s(t)] \\
&+ \sum_{s\in\mathcal{N}_S} \sum_{t\in\mathcal{T}} \sum_{a\in\mathcal{A}/\mathcal{A}_S} \sum_{c\in C} \sum_{e\in\mathcal{E}_c} \phi\delta[UE_{a,c}^{s,e}(t) - VE_{a,c}^{s,e}(t)] + \\
&\sum_{s\in\mathcal{N}_S} \sum_{t\in\mathcal{T}} \sum_{c\in C} \sum_{e\in\mathcal{E}_c} \sum_{a\in\mathcal{A}_C} \lambda_{N(a)}^t p_a^{ev}\delta[UE_{a,c}^{s,e}(t) - VE_{a,c}^{s,e}(t)] \\
&+ \sum_{t\in\mathcal{T}} \sum_{j\in\mathcal{P}_N} [a_j(p_j^g(t))^2 + b_j p_j^g(t)] + \sum_{t\in\mathcal{T}} \sum_{k\in\Gamma(0)} \mu(t)P_{0k}(t)
\end{aligned} \tag{34}$$

subject to constraints (7)–(12), (14)–(27) and (32), where $\boldsymbol{w} = \{\boldsymbol{y}, \boldsymbol{z}, \lambda, \boldsymbol{p}^{dc}\}$. It should be noted that charging load $p_j^{dc}$ are input parameters in **P1**, whereas they are decision variables here.

This problem can be interpreted as a fixed-point mapping $\Omega(\lambda) \coloneqq (\boldsymbol{y}, \boldsymbol{z}, \boldsymbol{p}^{dc}, \hat{\lambda})$ that identifies the optimal traffic-power flow pattern $(\boldsymbol{y}, \boldsymbol{z})$, the charging demand $\boldsymbol{p}^{dc}$, and the corresponding locational marginal prices (LMPs) $\hat{\lambda}$ under any given vector of LMPs $\lambda$. With a traffic-power flow pattern $(\boldsymbol{y}, \boldsymbol{z})$, LMPs $\hat{\lambda}$ are first retrieved from the mapping $\Omega(\cdot)$; then $\hat{\lambda}$ are fed into the centralized traffic-power systems, and the

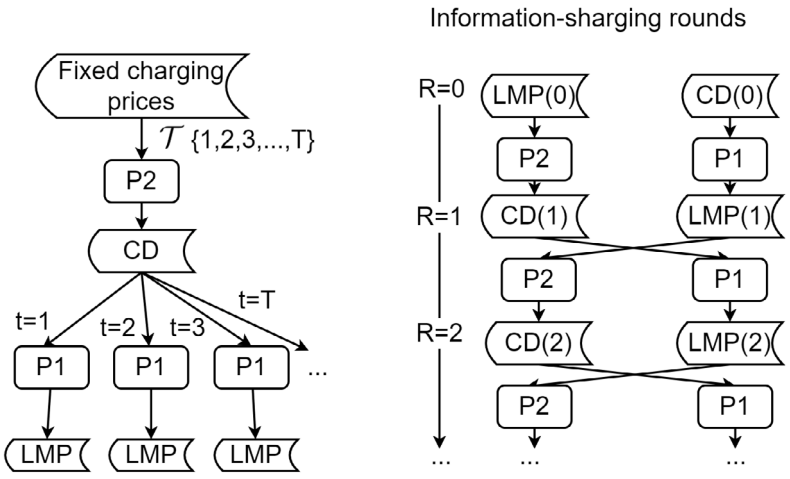


(a) Procedures of no information-sharing situation (b) Procedures of information-sharing situation

**Fig. 1.** Procedures of decentralized decision-making environments. CD: Charging demand of EVs; LMP: locational marginal price.

mapping $\Omega(\cdot)$ yields again an optimal traffic flow pattern $(\boldsymbol{y}, \boldsymbol{z})$, the charging demand $\boldsymbol{p}^{dc}$ and LMPs $\lambda$. This process constitutes a natural self-mapping mechanism and may converge to a fixed-point solution. This self-mapping problem is formulated as follows:

$$\boldsymbol{w} = \Omega(\boldsymbol{w})$$

where $\boldsymbol{w} = \{\boldsymbol{y}, \boldsymbol{z}, \lambda, \boldsymbol{p}^{dc}\} \in \{\Psi_T \times \Psi_P\}$.

To analyze the solution existence of the proposed model, Brouwer's fixed-point theorem is used. It states that a solution exists to the fixed-point problem $\boldsymbol{w} = \Omega(\boldsymbol{w})$ if the mapping $\Omega(\cdot)$ is continuous, and the set $\boldsymbol{w}$ is convex as well as compact. Because all variables are bounded and all constraints are convex in the optimal power flow problem **P1** and the optimal traffic flow problem **P2**, $\{\Psi_T \times \Psi_P\}$ is convex and compact. Ref. Xie et al. (2021) proved that **P1** for the PDN, mapping from traffic-power flow pattern $\{\boldsymbol{y}, \boldsymbol{z}, \boldsymbol{p}^{dc}\}$ to the optimal power flow solution and LMPs $\{\boldsymbol{z}, \lambda\}$ is continuous. For the ERNs, since **P2** is linear (Wang, Li, & Deng, 2024; Zhao, Li, & Deng, 2024), the mapping from traffic-power flow pattern $\{\boldsymbol{y}, \boldsymbol{z}, \lambda\}$ to the optimal traffic flow solution and charging demand $\{\boldsymbol{y}, \boldsymbol{p}^{dc}\}$ is continuous. Therefore, the composite mapping function $\Omega(\cdot)$ is, also, continuous.

Since variables $\lambda^t_{N(a)}$ can be only obtained after the optimal power flow $\boldsymbol{z}$ has been known, the proposed model cannot be solved directly by a common commercial solver. To solve the proposed self-mapping fixed-point problem, it is possible to construct an iterative algorithm with the following structure:

$$\boldsymbol{w}^{\chi+1} = \Omega(\boldsymbol{w}^{\chi})$$

The main procedures of the algorithm are listed in Algorithm 1. Continuity and monotonicity of the mapping operator of $\Omega(\cdot)$ is required to ensure the convergence of such an iterative algorithm (Cegielski, 2012; Deng, Deng, & Yang, 2024). However, since the optimal traffic flow problem **P2** in $\Omega(\cdot)$ has intersection delays that are not necessarily monotonically increasing as a function of traffic flow (Yperman, 2007), the convergence of $\boldsymbol{w}^{\chi}$ is not analytically ensured. Instead, convergence can be shown empirically via case studies.

**Algorithm 1:** An iterative algorithm

1 Initialization: Choose a convergence tolerance $\epsilon > 0$ and the maximum iteration number $I_{max}$. Let LMP vector $\lambda = 0$, objective value $\theta = 0, i = 0$ ;
2 Solve problem (34) with fixed LMP $\lambda$; Get the objective value $\theta^*$ and retrieve $\lambda^*$ from optimal power flow ;
3 **if** $|\theta - \theta^*| < \epsilon$ *for* $N$ *consecutive times* **then**
4 | terminate and return the solution of problem (34);
5 **else if** $i = I_{max}$ **then**
6 | terminate, report that the algorithm fails to converge and return the solution of problem (34);
7 **else** $i = i + 1, \theta = \theta^*, \lambda = \lambda^*$, go to Line 2;

## 4. Numerical examples and results

### 4.1. Case study and system configuration

The similar structures of the ERN (with modified road lengths) and the radial PDN (with added renewable generators) in Ref. Wei et al. (2018) are used to illustrate the proposed methods. The data used in the examples is briefly summarized in Appendix. More detailed data and parameters are available in Supplementary Material (*Supplementary material*, 2024). We consider 4 renewable distributed generators (DGs) and 4 conventional generators connected to 4 renewable FCS (charging link label: 65, 67, 70, 72) and 4 conventional FCS (66, 68, 69, 71), respectively. In this example, we consider similar assumptions to Ref. Zhang et al. (2020): (1) the DGs' outputs are assumed to be controllable which means the renewable power can be curtailed; (2) the available generation capacities of DGs are assumed to be given by proper forecasting methods, which provide the upper limits of the actual generation. The generation costs of both conventional and renewable DGs are detailed in Ref. Zhang et al. (2020).

### 4.2. Implementation note and results

The experiments were conducted on a computer equipped with an Intel Core i7-8700 3.2 GHz CPU and 32 GB of RAM. All problem-solving tasks were executed using the commercial software IBM ILOG CPLEX (version 12.6).

Theoretically, information could be exchanged for any number of rounds between system operators; however, it is reasonable to assume that they only exchange information once due to practical limitations, particularly concerning time.

Algorithm 1 is employed to compute the problem (34). To show the empirical convergence of the proposed algorithm, we analyzed 4

**Table 2**
Summary of the main results under different decision-making environments.

| Decision environments | | Cost ($) | | | | Generation and purchase (MWh) | | |
|---|---|---|---|---|---|---|---|---|
| | | Actual charging cost | Actual traffic cost | Power cost | Actual total cost | Electricity purchase | Conventional DG | Renewable DG (%) |
| Decentralized | No I.S. | 2556.78 | 11 770.78 | 3924.15 | 15 694.93 | 0.46 | 25.71 | 227.99(89.70%) |
| | I.S. | 245.21 | 9463.21 | 3924.15 | 13 387.36 | 0.46 | 25.71 | 228.01(89.71%) |
| Centralized | | 183.74 | 9821.34 | 3065.80 | 12 887.15 | 0.078 | 20.35 | 232.96(91.94%) |

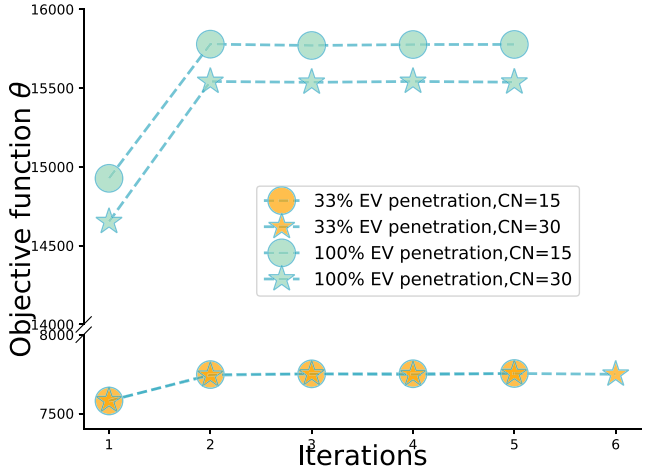


**Fig. 2.** Convergence performance of the proposed algorithm.

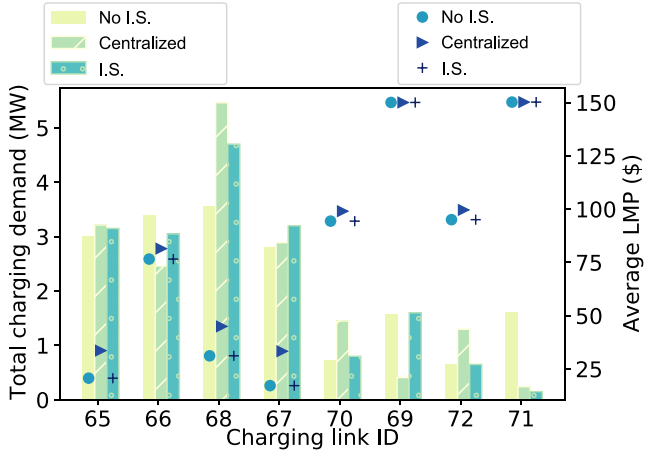


**Fig. 3.** Total charging demand and average LMP in FCSs.

scenarios. The spatial–temporal charging demand is the most important factor that impacts the interplays between the traffic-power systems, since it influences the locational marginal prices of power systems and the charging cost of traffic systems. Therefore, two EV penetration levels (33% and 100%) and two charging station sizes are studied. The former is directly related to the total charging demand, and the latter could provide more flexible charging choices for EV drivers from spatial and temporal distribution perspectives. The tolerance $\epsilon$ is set as 0.1% of the objective function and the maximum iteration number $I_{max} = 20$. Fig. 2 shows that the proposed algorithm can converge within 6 iterations in all studied scenarios.

Table 2 compares the results under the two decision-making environments. As it shows, we have the highest actual total cost $15694.93 when ERNs and PDNs operate independently. The total cost is 27.73% and 17.24% higher under the no information sharing (I.S.) situation, compared to full integration or sharing information, respectively. This

**Table 3**
Total charging demand in renewable and conventional FCSs (MWh)

| Environments | | RenewableFCS (%) | ConventionalFCS | Total |
|---|---|---|---|---|
| Decentralized | No I.S. | 7.175 (41.47%) | 10.125 | 17.3 |
| | I.S. | 7.8(45.09%) | 9.5 | 17.3 |
| Centralized | | 8.85(50.80%) | 8.57 | 17.42 |

is because under the no information sharing situation, the ERN operator only knows the fixed electricity price and has no information on the difference among FCSs and periods, which results in only travel time minimization being considered. This leads to the highest charging cost and power expenditure. When an ERN operator exchanges information once with a PDN operator before traffic assignment, a significant reduction in the actual charging cost of up to 90.41% can be achieved. This is because one round of information-sharing between the two operators can provide valuable information on the electricity price difference among FCSs and periods, although the information may not be exactly right. Such information can guide the ERN operator to minimize the travel time cost and charging cost. Under a fully integrated centralized environment, the actual charging cost and power cost could decrease by up to 92.81% and 21.87%, respectively. Moreover, Fig. 3 shows that the FCSs with lower charging prices are generally assigned with more charging demand, and this correlation is clearer under a centralized situation than the information-sharing situation. However, some exceptions can be observed, for instance, while the electricity price in FCS #68 is not the cheapest, it still maintains the most charging demand. This is because there is a trade-off between the saved charging cost and the extra time caused by detouring to the FCS with a cheaper charging price. Only when the charging price is cheap enough, EVs would detour to this particular FCS.

In addition, Table 2 shows that the centralized decision-making environment has the highest renewable energy adoption. This can be explained by two reasons: first, a part of charging demand is shifted from conventional FCSs to renewable FCSs as shown in Table 3. The charging demand in renewable FCSs increases from 41.47% to 45.09% if the decision environment changes from decentralized to centralized. More specifically, except FCS #68, the charging demands in the other three conventional FCSs (#66, #69 and #71) are shifted to renewable FCSs (#65, #67, #70 and #72) in varying degrees when the decision-making environments are centralized and information-sharing is on, as shown in Fig. 3. The second reason is that under the centralized decision-making environment, the system operator could properly assign the charging time and locations of EVs so as to alleviate the charging congestion in FCSs in peak hours and flatten the power demand curve. Note that the generation capacities of renewable DGs are limited in each period. Consequently, in peak hours, the expensive conventional energy could be replaced by cheap renewable energy. This can be verified by Figs. 4 and 5. For example, the congestion in charging links 65, 67 and 68 is significantly alleviated when two systems operate jointly, as shown in Fig. 4. As a result, the total power demand from the 3rd to the 9th time step is clipped to from the 13th to 26th time step, as shown in Fig. 5. In summary, the operator optimizes the charging demand in temporal and spatial aspects

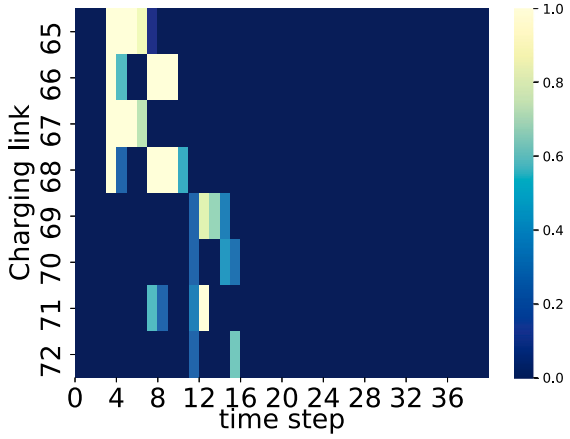


(a) Decentralized: No I.S.

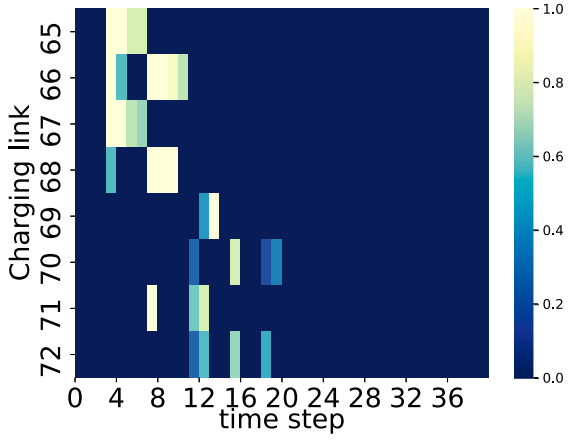


(b) Decentralized: I.S.

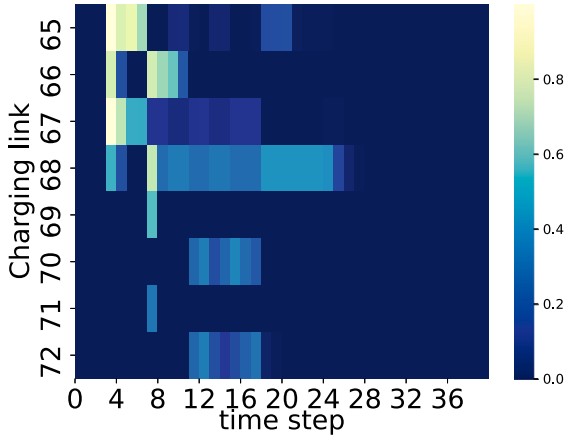


(c) Centralized

**Fig. 4.** Congestion level of FCS under different decision-making environments.

to promote renewable energy integration and, thus, the total cost is minimized.

## 5. Conclusion

This paper proposed a traffic-power system model to investigate the operational solution differences when the electric road network (ERN) and the power distribution network (PDN) operate independently and jointly. The model considered constraints from both ERNs and PDNs, such as road capacity, traffic flow capacity and ramp limit of generators. Within this model, an electric link transmission model (eLTM) was presented to solve the system optimal dynamic traffic assignment problem. A novel formulation was proposed to accommodate critical physical features of electric vehicles (EVs) and fast charging stations

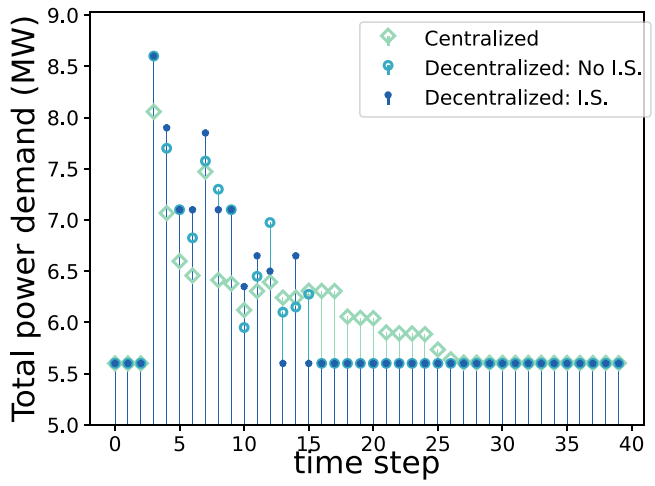


**Fig. 5.** The time distribution of the total power demand for the studied PDN.

(FCSs), such as, EV classes with different driving ranges, the initial state of charge (SoC) of EVs, the capacity of FCSs have been considered. Moreover, the charging process of EVs was explicitly modeled within the eLTM. The objective of a PDN operator was to minimize the power cost including power generation cost and purchase from the main grid. A numerical example including renewable and conventional generators was studied to illustrate the proposed models. The different decision-making environments were compared to investigate the corresponding operation and social benefits. From the results, we could observe that the charging cost was the highest under no information-sharing situation, since the ERN operator did not know the information on the electricity price difference among FCSs and periods. Even limitedly sharing information or operating jointly between ERNs and PDNs could significantly reduce the charging cost. The increased renewable energy adoption and the flattened power demand curve assisted in lowering charging cost, power cost and congestion level in FCSs, under a centralized situation. Both electricity price differences among FCSs and detouring time influenced the charging demand distribution.

This work can be extended in several directions: (1) It is interesting to investigate the proposed eLTM to solve the user equilibrium dynamic traffic assignment (UE-DTA) problem considering critical features of ERNs and FCSs. Although, Refs. Lv et al. (2019), Sun et al. (2020), Zhou et al. (2021) claimed that they have solved UE-DTA considering EVs, they oversimplified the critical features of ERNs and FCSs, as shown in Table 1. Therefore, how to solve this problem is still challenging. (2) The proposed models can be easily extended to investigate how the failure spreads between the interdependent traffic-power systems. (3) It is also interesting to investigate how to coordinate the charging demand so as to maximize renewable energy adoption considering the security constraints and the weather conditions.

## CRediT authorship contribution statement

**Hongping Wang:** Writing – original draft, Visualization, Software, Methodology, Investigation, Formal analysis, Data curation, Conceptualization. **Adam Abdin:** Writing – review & editing, Validation, Software, Methodology, Supervision. **Yi-Ping Fang:** Writing – review & editing, Validation, Supervision, Investigation, Conceptualization. **Jakob Puchinger:** Writing – review & editing, Validation, Formal analysis. **Enrico Zio:** Writing – review & editing, Validation, Supervision, Project administration, Investigation, Conceptualization.

## Data availability

Data will be made available on request.

**Table A.4**
Connections between charging links and Buses.

| Charging link | Bus |
|---|---|
| 65 | 1 |
| 66 | 2 |
| 67 | 4 |
| 68 | 3 |
| 69 | 6 |
| 70 | 5 |
| 71 | 8 |
| 72 | 7 |

**Table A.5**
Parameters of the studied traffic-power system.

| Parameters | Values |
|---|---|
| $v_f$ (m/h) | 50 |
| $k_{jam}$(veh/m) | 214 |
| $\delta$ (min) | 6 |
| $q_{max}$ (veh/h/lane) | 2160 |
| $p_a^{ev}$ (kW) | 50 |
| $\eta$ (kMh/mile) | 0.25 |
| $\phi$ ($/h) | 10 |
| $C$ | 1 |
| $E_c$ | 20 |
| $B_c$ (kWh) | 26 |
| $NC_a(t)$ | 15 |
| $\alpha_a^l$ (ELs/$\delta$) | 4 |

**Table A.6**
Parameters of the studied electrified road network.

| Road | Type-1 | Type-2 | Type-3 | Type-4 | Charging |
|---|---|---|---|---|---|
| $\nu_a$ | 2 | 2 | 4 | 6 | 0 |
| $\beta_a$ | 2 | 2 | 4 | 6 | 0 |
| $\rho_a$ | 2 | 2 | 4 | 6 | 0 |

**Table A.7**
O-D pairs and their trip rates (in P.U.)

| O-D pair | Conventional vehicles | EV | O-D pair | Conventional vehicles | EV |
|---|---|---|---|---|---|
| 21–28 | 30 | 15 | 22–28 | 30 | 15 |
| 21–26 | 60 | 30 | 22–26 | 50 | 25 |
| 21–24 | 40 | 20 | 22–24 | 40 | 20 |
| 21–25 | 40 | 20 | 22–25 | 50 | 25 |
| 23–27 | 50 | 15 | 23–26 | 40 | 20 |
| 23–25 | 40 | 20 | | | |

## Acknowledgment

Hongping Wang sincerely thanks the support of the Fundamental research funds for the central universities (2023RC37).

## Appendix. Data description

A modified electrified road network (Wei et al., 2018) and a power distribution network are used to illustrate the proposed methods. Figs. A.6 and A.7 show the modified road network and power network. As shown in Fig. A.6, there is one type of charger in each FCS. The green mark on charging links and generators represents the corresponding FCSs and generators powered by renewable energy. The detailed connections between charging links and buses are listed in Table A.4. The parameters used in this paper are listed in Tables A.5 and A.6. For simplicity, we assume there is one type of EV and its battery capacity is 25 KWh and its maximum energy level is 20. Total traffic demand is listed in Table A.7. More detailed data on the studied road network and power network are available in Supplementary Material (*Supplementary material*, 2024).

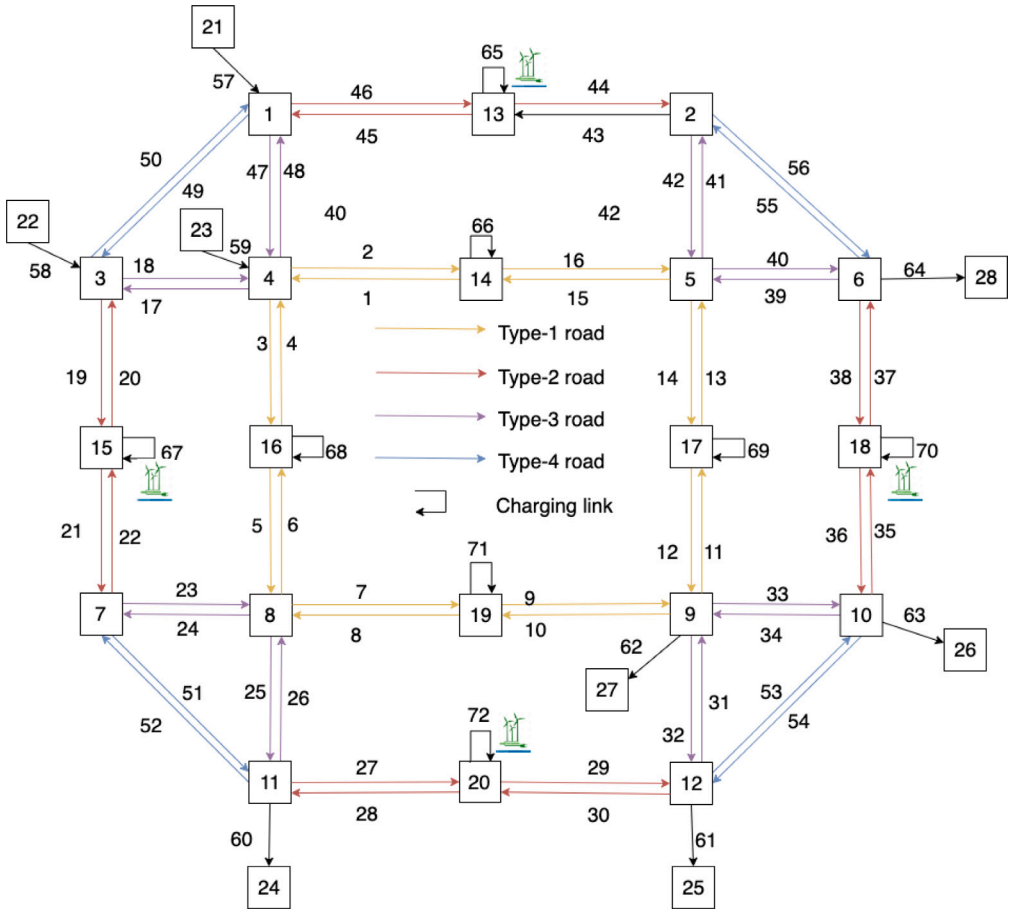


**Fig. A.6.** The studied electrified road network (Wei et al., 2018).

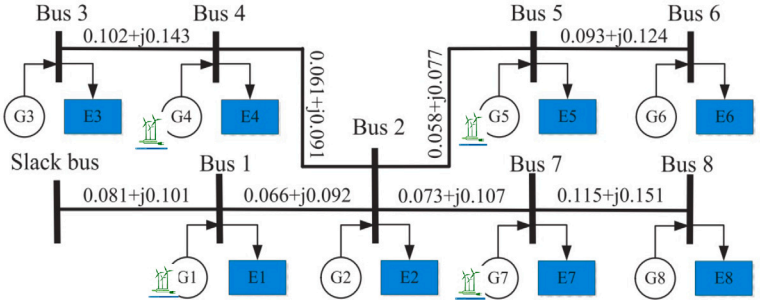


**Fig. A.7.** The studied Power distribution network (Wei et al., 2018).

## References


Alqahtani, M., Scott, M. J., & Hu, M. (2022). Dynamic energy scheduling and routing of a large fleet of electric vehicles using multi-agent reinforcement learning. *Computers & Industrial Engineering*, *169*, Article 108180.

Bai, Z., Yang, L., Fu, C., Liu, Z., He, Z., & Zhu, N. (2022). A robust approach to integrated wireless charging infrastructure design and bus fleet size optimization. *Computers & Industrial Engineering*, *168*, Article 108046.

Basso, R., Kulcsár, B., Sanchez-Diaz, I., & Qu, X. (2022). Dynamic stochastic electric vehicle routing with safe reinforcement learning. *Transportation Research Part E: Logistics and Transportation Review*, *157*, Article 102496.

Bi, J., Wang, Y., & Zhang, J. (2018). A data-based model for driving distance estimation of battery electric logistics vehicles. *EURASIP Journal on Wireless Communications and Networking*, *2018*, 1–13.

Cegielski, A. (2012). *Iterative methods for fixed point problems in Hilbert spaces*: *vol. 2057*, Springer.

Chen, X., & Deng, Y. (2024). Evidential software risk assessment model on ordered frame of discernment. *Expert Systems with Applications*, *250*, Article 123786.

Chen, R., Qian, X., Miao, L., & Ukkusuri, S. V. (2020). Optimal charging facility location and capacity for electric vehicles considering route choice and charging time equilibrium. *Computers & Operations Research*, *113*, Article 104776.

Deng, J., Deng, Y., & Yang, J.-B. (2024). Random permutation set reasoning. *IEEE Transactions on Pattern Analysis and Machine Intelligence*, http://dx.doi.org/10.1109/TPAMI.2024.3438349.

Ding, Z., Teng, F., Sarikprueck, P., & Hu, Z. (2020). Technical review on advanced approaches for electric vehicle charging demand management, part II: Applications in transportation system coordination and infrastructure planning. *IEEE Transactions on Industry Applications*, *56*(5), 5695–5703.

Dunckley, J. (2018). *Electric vehicle driving, charging, and load shape analysis: A deep dive into where, when, and how much salt river project (SRP) electric vehicle customers charge*. Electric Power Research Institute.

Erdoğan, B., Tural, M. K., & Khoei, A. A. (2023). Finding an energy efficient path for plug-in electric vehicles with speed optimization and travel time restrictions. *Computers & Industrial Engineering*, *176*, Article 108987.

Geng, L., Lu, Z., He, L., Zhang, J., Li, X., & Guo, X. (2019). Smart charging management system for electric vehicles in coupled transportation and power distribution systems. *Energy*, *189*, Article 116275.

Hariri, A.-M., Hejazi, M. A., & Hashemi-Dezaki, H. (2021). Investigation of impacts of plug-in hybrid electric vehicles' stochastic characteristics modeling on smart grid reliability under different charging scenarios. *Journal of Cleaner Production*, *287*, Article 125500.

He, Y., Liu, Z., & Song, Z. (2020). Optimal charging scheduling and management for a fast-charging battery electric bus system. *Transportation Research Part E: Logistics and Transportation Review*, *142*, Article 102056.

He, F., Yin, Y., & Lawphongpanich, S. (2014). Network equilibrium models with battery electric vehicles. *Transportation Research, Part B (Methodological)*, *67*, 306–319.

Hiermann, G., Hartl, R. F., Puchinger, J., & Vidal, T. (2019). Routing a mix of conventional, plug-in hybrid, and electric vehicles. *European Journal of Operational Research*, *272*(1), 235–248.

International Energy Agency (IEA) (2020). *Global EV outlook 2020*: *Tech. rep*, IEA.

Islam, M. R., Lu, H., Hossain, M. J., & Li, L. (2020). Optimal coordination of electric vehicles and distributed generators for voltage unbalance and neutral current compensation. *IEEE Transactions on Industry Applications*, *57*(1), 1069–1080.

Kchaou-Boujelben, M., & Gicquel, C. (2020). Locating electric vehicle charging stations under uncertain battery energy status and power consumption. *Computers & Industrial Engineering*, *149*, Article 106752.

Kostopoulos, E. D., Spyropoulos, G. C., & Kaldellis, J. K. (2020). Real-world study for the optimal charging of electric vehicles. *Energy Reports*, *6*, 418–426.

Li, Y.-F., Zhao, W., Zhang, C., Ye, J., & He, H. (2024). A study on the prediction of service reliability of wireless telecommunication system via distribution regression. *Reliability Engineering & System Safety*, *250*, Article 110291.

Liu, Z., Wu, Q., Ma, K., Shahidehpour, M., Xue, Y., & Huang, S. (2018). Two-stage optimal scheduling of electric vehicle charging based on transactive control. *IEEE Transactions on Smart Grid*, *10*(3), 2948–2958.

Liu, H., Zou, Y., Chen, Y., & Long, J. (2021). Optimal locations and electricity prices for dynamic wireless charging links of electric vehicles for sustainable transportation. *Transportation Research Part E: Logistics and Transportation Review*, *152*, Article 102187.

Long, J., & Szeto, W. Y. (2019). Link-based system optimum dynamic traffic assignment problems in general networks. *Operations Research*, *67*(1), 167–182.

Lv, S., Wei, Z., Chen, S., Sun, G., & Wang, D. (2021). Integrated demand response for congestion alleviation in coupled power and transportation networks. *Applied Energy*, *283*, Article 116206.

Lv, S., Wei, Z., Sun, G., Chen, S., & Zang, H. (2019). Optimal power and semi-dynamic traffic flow in urban electrified transportation networks. *IEEE Transactions on Smart Grid*, *11*(3), 1854–1865.

Newell, G. F. (1993a). A simplified theory of kinematic waves in highway traffic, part I: General theory. *Transportation Research, Part B (Methodological)*, *27*(4), 281–287.

Newell, G. F. (1993b). A simplified theory of kinematic waves in highway traffic, part II: Queueing at freeway bottlenecks. *Transportation Research, Part B (Methodological)*, *27*(4), 289–303.

Patnaik, L., Praneeth, A., & Williamson, S. S. (2018). A closed-loop constant-temperature constant-voltage charging technique to reduce charge time of lithium-ion batteries. *IEEE Transactions on Industrial Electronics*, *66*(2), 1059–1067.

Qian, T., Shao, C., Wang, X., & Shahidehpour, M. (2019). Deep reinforcement learning for EV charging navigation by coordinating smart grid and intelligent transportation system. *IEEE Transactions on Smart Grid*, *11*(2), 1714–1723.

Quddus, M. A., Kabli, M., & Marufuzzaman, M. (2019). Modeling electric vehicle charging station expansion with an integration of renewable energy and Vehicle-to-Grid sources. *Transportation Research Part E: Logistics and Transportation Review*, *128*, 251–279.

Rossi, F., Iglesias, R., Alizadeh, M., & Pavone, M. (2019). On the interaction between Autonomous Mobility-on-Demand systems and the power network: Models and coordination algorithms. *IEEE Transactions on Control of Network Systems*, *7*(1), 384–397.

Shin, M., Choi, D.-H., & Kim, J. (2019). Cooperative management for PV/ESS-enabled electric vehicle charging stations: A multiagent deep reinforcement learning approach. *IEEE Transactions on Industrial Informatics*, *16*(5), 3493–3503.

Sun, G., Li, G., Xia, S., Shahidehpour, M., Lu, X., & Chan, K. W. (2020). ALADIN-based coordinated operation of power distribution and traffic networks with electric vehicles. *IEEE Transactions on Industry Applications*, *56*(5), 5944–5954.

Supplementary material. (2024). https://github.com/lucky105/Coordinating-dynamic-traffic-power-systems-under-decentralized-centralized-and-formation-sharing. (Accessed December 2023).

Tahami, H., Rabadi, G., & Haouari, M. (2020). Exact approaches for routing capacitated electric vehicles. *Transportation Research Part E: Logistics and Transportation Review*, *144*, Article 102126.

Tang, D., & Wang, P. (2016). Nodal impact assessment and alleviation of moving electric vehicle loads: From traffic flow to power flow. *IEEE Transactions on Power Systems*, *31*(6), 4231–4242.

Teng, F., Ding, Z., Hu, Z., & Sarikprueck, P. (2020). Technical review on advanced approaches for electric vehicle charging demand management, part I: Applications in electric power market and renewable energy integration. *IEEE Transactions on Industry Applications*, *56*(5), 5684–5694.

Tran, C. Q., Keyvan-Ekbatani, M., Ngoduy, D., & Watling, D. (2021). Stochasticity and environmental cost inclusion for electric vehicles fast-charging facility deployment. *Transportation Research Part E: Logistics and Transportation Review*, *154*, Article 102460.

Vosooghi, R., Puchinger, J., Bischoff, J., Jankovic, M., & Vouillon, A. (2020). Shared autonomous electric vehicle service performance: Assessing the impact of charging infrastructure. *Transportation Research Part D: Transport and Environment*, *81*, Article 102283.

Wang, B., Dehghanian, P., Wang, S., & Mitolo, M. (2019). Electrical safety considerations in large-scale electric vehicle charging stations. *IEEE Transactions on Industry Applications*, *55*(6), 6603–6612.

Wang, H., Fang, Y.-P., & Zio, E. (2021). Risk assessment of an electrical power system considering the influence of traffic congestion on a hypothetical scenario of electrified transportation system in New York state. *IEEE Transactions on Intelligent Transportation Systems*, *22*(1), 142–155.

Wang, H., Fang, Y.-P., & Zio, E. (2022). Resilience-oriented optimal post-disruption reconfiguration for coupled traffic-power systems. *Reliability Engineering & System Safety*, *222*, Article 108408.

Wang, Y., Li, Z., & Deng, Y. (2024). A new orthogonal sum in random permutation set. *Fuzzy Sets and Systems*, *490*, Article 109034.

Wang, Q., Liu, X., Du, J., & Kong, F. (2016). Smart charging for electric vehicles: A survey from the algorithmic perspective. *IEEE Communications Surveys & Tutorials*, *18*(2), 1500–1517.

Wang, X., Shahidehpour, M., Jiang, C., & Li, Z. (2018). Coordinated planning strategy for electric vehicle charging stations and coupled traffic-electric networks. *IEEE Transactions on Power Systems*, *34*(1), 268–279.

Wei, C., Tang, D., & Hong, L. (2021). Propagation analysis and cascading effects of charging station failure considering dynamic traffic assignment. In *2021 IEEE sustainable power and energy conference* (pp. 3538–3543). IEEE.

Wei, W., Wu, L., Wang, J., & Mei, S. (2018). Network equilibrium of coupled transportation and power distribution systems. *IEEE Transactions on Smart Grid*, *9*(6), 6764–6779.

Xie, S., Hu, Z., Wang, J., & Chen, Y. (2020). The optimal planning of smart multi-energy systems incorporating transportation, natural gas and active distribution networks. *Applied Energy*, *269*, Article 115006.

Xie, S., Xu, Y., & Zheng, X. (2021). On dynamic network equilibrium of a coupled power and transportation network. *IEEE Transactions on Smart Grid*, *13*(2), 1398–1411.

Yan, H., Zhao, T., & Guan, Z. (2024). Proactive resilience enhancement of power systems with link transmission model-based dynamic traffic assignment among electric vehicles. *CSEE Journal of Power and Energy Systems*.

Yang, T., Guo, Q., Xu, L., & Sun, H. (2021). Dynamic pricing for integrated energy-traffic systems from a cyber-physical-human perspective. *Renewable and Sustainable Energy Reviews*, *136*, Article 110419.

Yang, X.-G., Zhang, G., Ge, S., & Wang, C.-Y. (2018). Fast charging of lithium-ion batteries at all temperatures. *Proceedings of the National Academy of Sciences*, *115*(28), 7266–7271.

Yazdekhasti, A., Jazi, M. A., & Ma, J. (2021). Electric vehicle charging station location determination with consideration of routing selection policies and driver's risk preference. *Computers & Industrial Engineering*, *162*, Article 107674.

Yperman, I. (2007). The link transmission model for dynamic network loading.

Zahedmanesh, A., Muttaqi, K. M., & Sutanto, D. (2020). Coordinated charging control of electric vehicles while improving power quality in power grids using a hierarchical decision-making approach. *IEEE Transactions on Vehicular Technology*, *69*(11), 12585–12596.

Zhang, H., Hu, Z., & Song, Y. (2020). Power and transport nexus: Routing electric vehicles to promote renewable power integration. *IEEE Transactions on Smart Grid*, *11*(4), 3291–3301.

Zhang, L., Liu, Z., Yu, L., Fang, K., Yao, B., & Yu, B. (2022). Routing optimization of shared autonomous electric vehicles under uncertain travel time and uncertain service time. *Transportation Research Part E: Logistics and Transportation Review*, *157*, Article 102548.

Zhang, L., Wang, S., & Qu, X. (2021). Optimal electric bus fleet scheduling considering battery degradation and non-linear charging profile. *Transportation Research Part E: Logistics and Transportation Review*, *154*, Article 102445.

Zhao, T., Li, Z., & Deng, Y. (2024). Linearity in deng entropy. *Chaos, Solitons & Fractals*, *178*, Article 114388.

Zhao, T., Yan, H., Liu, X., & Ding, Z. (2022). Congestion-aware dynamic optimal traffic power flow in coupled transportation power systems. *IEEE Transactions on Industrial Informatics*, *19*(2), 1833–1843.

Zheng, Y., Niu, S., Shang, Y., Shao, Z., & Jian, L. (2019). Integrating plug-in electric vehicles into power grids: A comprehensive review on power interaction mode, scheduling methodology and mathematical foundation. *Renewable and Sustainable Energy Reviews*, *112*, 424–439.

Zhou, Z., Zhang, X., Guo, Q., & Sun, H. (2021). Analyzing power and dynamic traffic flows in coupled power and transportation networks. *Renewable and Sustainable Energy Reviews*, *135*, Article 110083.